TECHNICAL PROGRESS REPORT

A: COVER SHEET

Name of Submitting Organization: Nuonics, Inc.
Address of Submitting Organization: 1025 S. Semoran Blvd, Suite 1093, Winter Park, FL 32792
Tel/Fax: 407-379-0164

Name & Address of Sub-Contractors: (a) University of Central Florida, 4000 Central Florida Blvd., CREOL Bldg, Orlando, FL 32816-2700 and (b) AppliCote Associates, LLC, 3259 Progress Drive A, Orlando, FL 32826.

DOE Award No.: DE-FC26-03NT41923

Project Title: Ultra-High Temperature Sensors Based on Optical Property Modulation and Vibration-Tolerant Interferometry

Dated: July 22, 2005

Principal Author: Dr. Nabeel A. Riza (email: nriza@aol.com)

Period Covered by Report: Jan. 1, 2005 – June 30, 2005.
Type of Report: Semi-Annual Technical Progress Report

B: ABSTRACT

The goals of the first six months of this project were to begin laying the foundations for both the SiC front-end optical chip fabrication techniques for high pressure gas species sensing as well as the design, assembly, and test of a portable high pressure high temperature calibration test cell chamber for introducing gas species. This calibration cell will be used in the remaining months for proposed first stage high pressure high temperature gas species sensor experimentation and data processing. All these goals have been achieved and are described in detail in the report. Both design process and diagrams for the mechanical elements as well as the optical systems are provided. Photographs of the fabricated calibration test chamber cell, the optical sensor setup with the calibration cell, the SiC sample chip holder, and relevant signal processing mathematics are provided. Initial experimental data from both the optical sensor and fabricated test gas species SiC chips is provided. The design and experimentation results are summarized to give positive conclusions on the proposed novel high temperature high pressure gas species detection optical sensor technology.

C: TABLE OF CONTENTS

D: LIST OF GRAPHICAL MATERIALS

E: INTRODUCTION

The purpose of this project is to develop a science base to fabricate sensors for ultra high temperature fossil fuel applications. The sensors proposed are based on the principle of the Optical Path Length (OPL) variation in a medium owing to the dependence of the optical property (e.g., refractive index) of a high temperature material, such as silicon carbide (SiC), on the temperature, pressure, or species concentration. These three thermodynamic variables can be measured by a single sensor if we understand how they individually change the refractive index of the sensor material. Since these changes can be very small, a high accuracy optical signal processing scheme is proposed for working in unison with the remote SiC sensor frontend. Specifically, a vibration-tolerant interferometric technique capable of measuring the changes in OPL with sub-nanoscale accuracy and at a high speed is investigated in this project. The proposed novel sensor technique will thus enable us to measure the desired variables remotely, accurately and rapidly.

Remote interrogation of the sensor by using a laser beam will eliminate the complications associated with electrical signal-based sensors in high temperature applications. The complications in such conventional sensors include (i) melting of the solder joint between the sensor device and the bonding wire, (ii) requirement of high temperature insulation for the electrical wires connecting the device to the electrical signal processing unit, and (iii) inconvenience in mounting or embedding the device in rotating components such as the turbine blades. A high speed optical interferometer can respond to the changes in the thermodynamic variables rapidly at microsecond speeds allowing real-time control of the combustion process.

Since a passive sensor frontend chip is proposed, any optically transparent high temperature material, such as a single crystal silicon carbide, diamond or sapphire, can be used as the sensor

chip material. Such a passive sensor chip can be custom fabricated for specific gas species detection and produced at low cost in a small (sub-millimeter) size and can be readily embedded in a small hole at the surface of any structure by using the thermal expansion/contraction stress-based fitting method. The structure could be a stationary or rotating component containing the sensor at a convenient location providing remote accessibility to the probe laser beam for interferometry.

Note that the leading fiber-optic sensors such as using fiber Fabry-Perot interference or in-fiber Bragg Gratings with wavelength-based processing require costly environmental protection of the light delivery and light return fiber [1-3]. This is because the fiber intrinsically contains both the sensing zone that must react to the changing environmental conditions (e.g., temperature) and the light delivery fiber that should stay protected and essentially unaffected from changing environmental effects (e.g., changing stresses in the long lengths of the delivery fiber could cause unexpectedly high bending losses leading to loss of detection signal). It is well known that standard low loss single mode optical fibers (SMFs) are made of glass, with transition temperatures around 475 °C, leading to unwanted softening of glass at higher temperatures, such as needed in DOE applications. Thus, there exists a dilemma for the sensor design engineer using the mentioned fiber-optic sensors. In our proposed sensor, this dilemma is removed as a free-space laser beam reads sensing parameters off the SiC sensor chip, thus producing no physical contact between the harsh environment and the light delivery and processing optics. In effect, one can imagine many low cost SiC optical chips distributed in the desired sensing zone where a scanning free-space laser beam rapidly engages these sensor frontend chips to produce signals for later data processing and environmental parameter recovery. In effect, a truly non-invasive distributed optical sensor is realized.

F: EXECUTIVE SUMMARY

Accomplishments during the first six months of this project have been achieved on three fronts, namely; design, fabrication, and preliminary testing of proposed gas species optical sensor using SiC optical chip and interface optics. One objective was to build a custom portable calibration test chamber for introducing gas species at high temperature (up to 500°C) and high pressure (up to 50 bars) for initial testing of the proposed sensor and its related custom fabricated SiC optical chips. This chamber must be capable of holding a SiC optical chip window that can interface with a freespace laser beam coming from the optical sensor interface. Such a chamber has been successfully designed and the detailed mechanical design is presented in this report. The chamber is designed to hold up-to two inch diameter SiC chips and can be readily inserted into prototype and commercial Integrated Gasification Combined Cycle (IGCC) systems. This portable chamber can therefore act as a general test instrument for various type of chip-based optical sensing scenarios such as DOE related initiatives.

Another first phase project objective was to initiate the fabrication processes to enable SiC optical chips for gas species detection. We have taken two parallel approaches to solve this problem. First, we are tuning the chemistry of the SiC chip by doping and two we are using selective gas trapping structures including the SiC chip lattice, grain boundaries and vacancies/voids. Aluminum has been laser doped into 6H-SiC chip to tune the refractive index response to primarily oxygen, a safe gas species to test. As an on-going first step, we have chosen the Nitrogen gas for species sensing as Nitrogen is a safe gas to use for initial tests of gas doping effects. We have successfully doped SiC with nitrogen and have detected a change in refractive index in the material result from electron donation to SiC.

The related first phase project objective was to design, fabricate, and conduct preliminary tests on the optical interface with the fabricated gas Calibration cell. The baseline interface was designed and tested using a 1550 nm tunable laser. Initial effects of gas pressure on the optical sensor design have been studied indicating how the sensor can be designed to be robust (i.e., optical chip does not break) and optical readings can be used to measure pressure. In addition, studies show that the chip size can be reduced and thickness increased to make optical measurements pressure independent and thus suitable for independent gas species measurement.

G: EXPERIMENTAL RESULTS

G.1 Construction of Test Equipment:

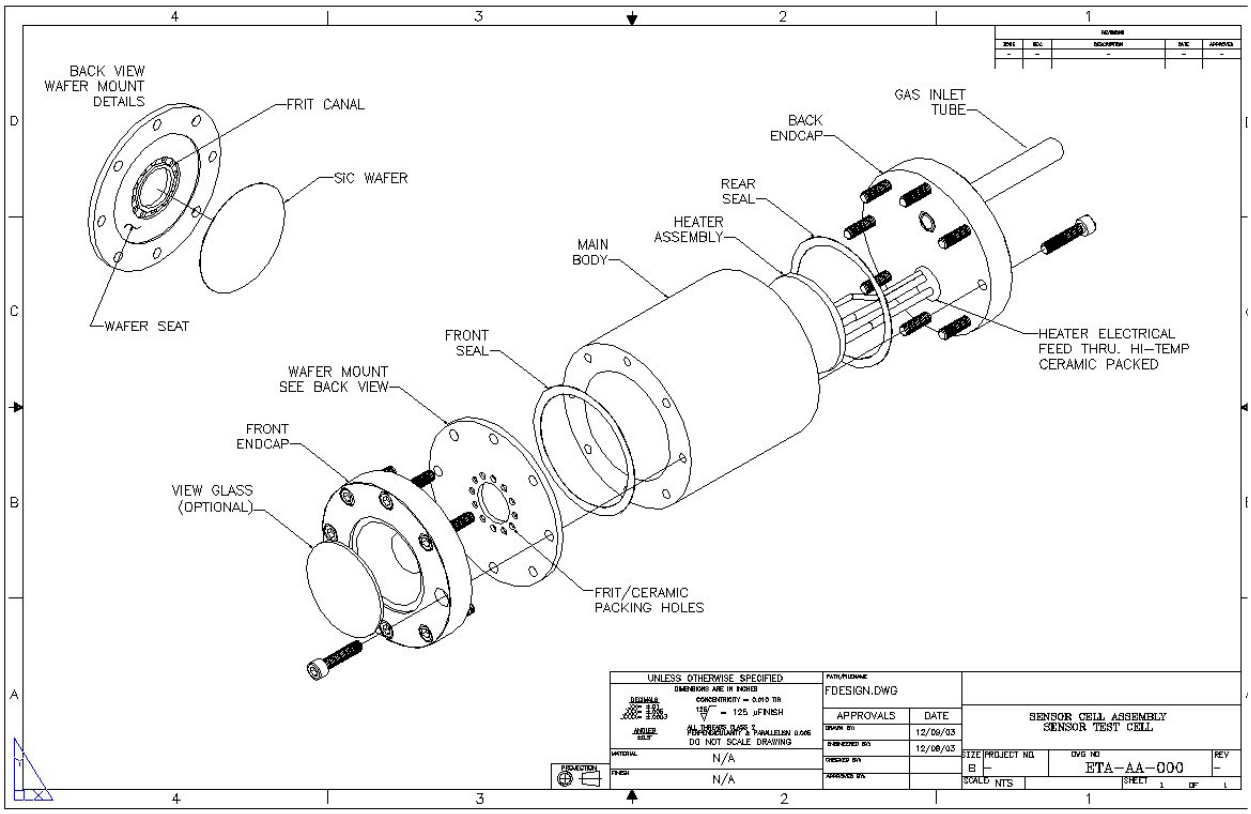

Figure 1. Exploded View of the Calibration Test Cell.

A calibration test cell design has evolved from separate cell concepts, where three cells were specifically designed for dedicated pressure, temperature and chemical sensing, to one integrated cell capable of producing environments for all three variables. The laboratory calibration test cell is designed for insertion into prototype and commercial IGCC systems. This calibration test cell is completed for pressure testing and a schematic is shown in Figure 1. A salient feature of this test cell is the use of glass frit for sealing of 2 inch (50 mm) diameter Silicon (Si) and SiC wafers for leak prevention at high temperatures. During the initial pressure testing at room temperature, an RTV at sealant will be used to allow easy debugging. The deflection diameter of the wafer will first be constrained to 0.75 inch (19 mm) diameter.

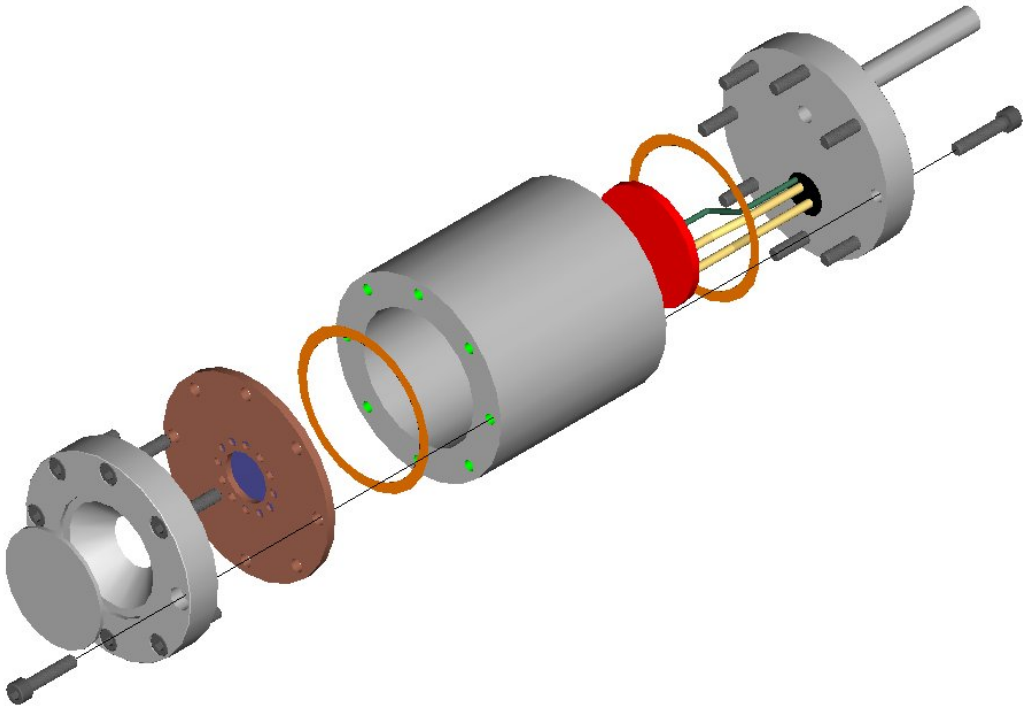

Figure 1 (Continued). Exploded View of the Calibration Test Cell.

Computer-based Finite Element Analysis (FEA) has been used to model the theoretical deflection of first Silicon then SiC chips under pressures up to 50 bar (725 psi) (Note that 1 bar = 14.5 psi). The accuracy of the model was first analyzed using parameters for conventional SAE 1330 steel; the model successfully predicted all facets of the material's behavior. In this study, Silicon is used first as a reference material since Silicon diaphragm technology based on electrical property changes of the device (e.g., gap capacitance) is well established commercially for pressure sensing. The model and our initial optical sensing results can be compared to earlier published data. The FEA model(s) also have the capability to predict defect sites, which can lead to catastrophic failure. The FEA conducted maximum predicted deflections at 700 psi are given in Table 1.

Table 1. FEA Model Predictions for 0.75inch diameter chips.

Material	**Deflection (in.)**	**Deflection (cm)**
Silicon	0.04806	0.122072
Silicon Carbide	0.040050	0.101727

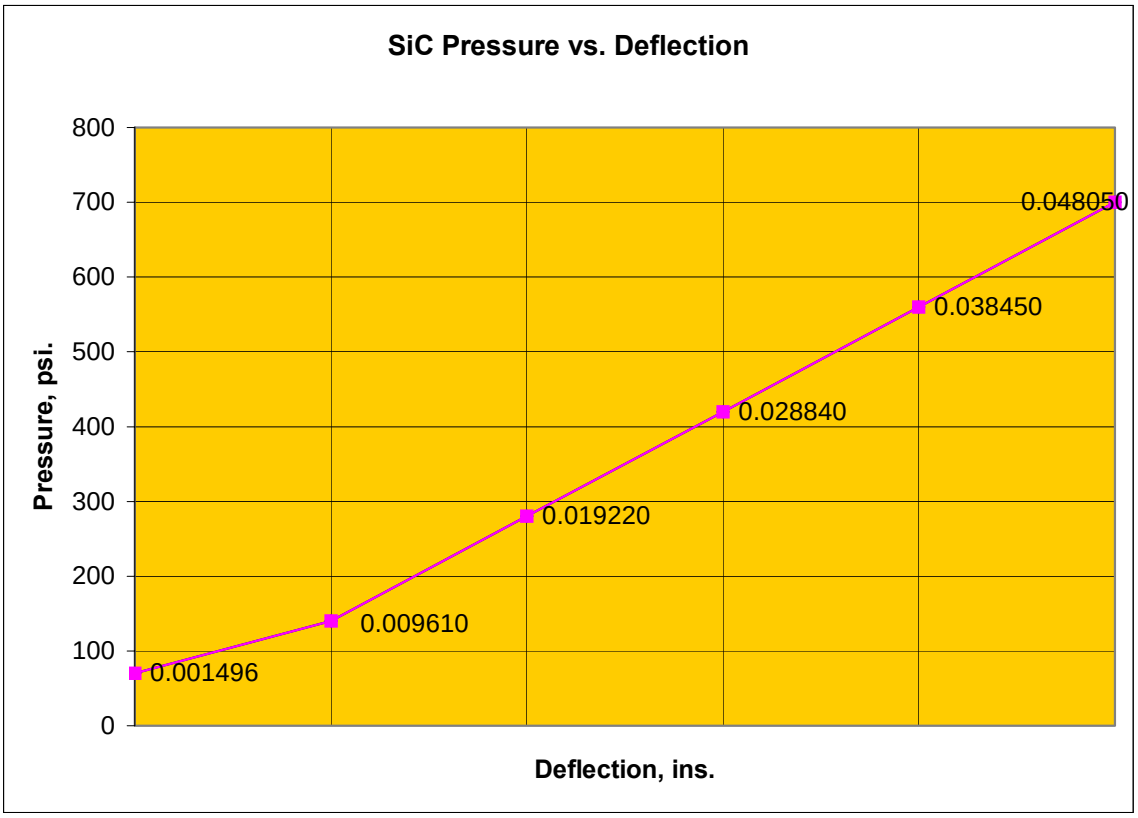

Fig.2. The modeled deformation of the 0.75 inch SiC chip as a function of pressure is linear; hence this deformation is elastic.

Figure 2 shows that deformation of the silicon carbide disc as a function of pressure is linear; this deformation is elastic. SiC wafers are on order while initial testing Silicon wafers have been procured and are characterized as follows:

Thickness: 300+/-25 microns
Surface: Both sides polished (3 Angstrom finish)
Crystallographic orientation: 100
Chemistry: Boron doped (p-type semiconductor)
Diameter: 50.8 +/-0.3 mm diameter

G.2 Fabrication and Testing of SiC Chip for Gas Species Detection:

The calibration test cell is being outfitted with a heater to accommodate for chemical species testing. Our intent is to characterize optical property changes in SiC induced by chemical interactions. This approach differs from the study of electrical property changes caused by changes in SiC interface states induced by chemical interactions [4]. Our team is exploring

methods to fabricate gas selective chemical sensors. Our approach 1 is to tune the chemistry of the SiC chip by doping and Approach 2 is to use selective gas trapping structures including the SiC chip lattice, grain boundaries and vacancies/voids. The present section discusses Approach 1 where laser doping is used to tune the chemical responsiveness and the refractive index. Aluminum has been laser doped into 6H-SiC chip to tune the refractive index response to primarily oxygen. Laser doping with nitrogen will be conducted next to simulate refractive index changes for near surface lattice absorption for nitrogen gas sensing. Refractive index will next be measured on Aluminum and nitrogen doped samples and correlated to dopant concentration.

We have successfully doped SiC with nitrogen and have detected a change in refractive index in the material result from electron donation to SiC. This fact, in addition to safety requirements has led to the use of nitrogen as a first test gas to analyze the chemical sensing capability of SiC. Argon will be the next gas to be studied to analysis for mass discrimination. In approach 1, SiC can be doped for additional selectivity. After demonstrating the proof –of-concept, the gaseous precursor gases and reaction product gases from IGCC power generation will be used as feed gases for sensing analysis after the proper safety precautions are implemented. These gases, including hydrogen, carbon monoxide, carbon dioxide, methane, etc., will be mixed in low concentration with inert gases in an attempt to create safe noncombustible gas solutions. Low temperature in situ calibration studies will require a Fourier Transform Infrared Spectrometer. In-situ characterization of the chemical and structural transitions of SiC during sensing will require the use of instrumentation such as a Field Emission Scanning Electron Microscope integrated with Focused Ion Beam Milling and Energy Dispersive Spectra.

Doping of SiC for Modulation of Refractive Index and Analysis of the Dopant level Using Secondary Ion Mass Spectroscopy (SIMS):

We have doped two SiC samples A and B by using a laser doping technique. The thicknesses of samples A and B were measured to be 380 μm and 420 μm respectively and the sensor area was 7.9 mm. The samples were analyzed for their dopant contents because dopant atoms affect the refractive index of dielectrics. As-grown single-crystal SiC wafers are known to contain unintentional dopants. The depth profiles of dopant concentration were acquired with a

Perkin-Elmer PHI 6600 SIMS system using a 6 keV Duoplasmatron (oxygen) primary ion beam with positive secondary acquisition and a 5 keV Cesium primary ion beam with negative secondary acquisition. The current intensity was set at 118 nA during oxygen sputtering and at 153 nA during Cs sputtering. The raster size was 300x300 μm^2. Gating was set at 65% for depth profiles and at 55% for mass surveys. The neutralizer was used during the analysis for charge compensation.

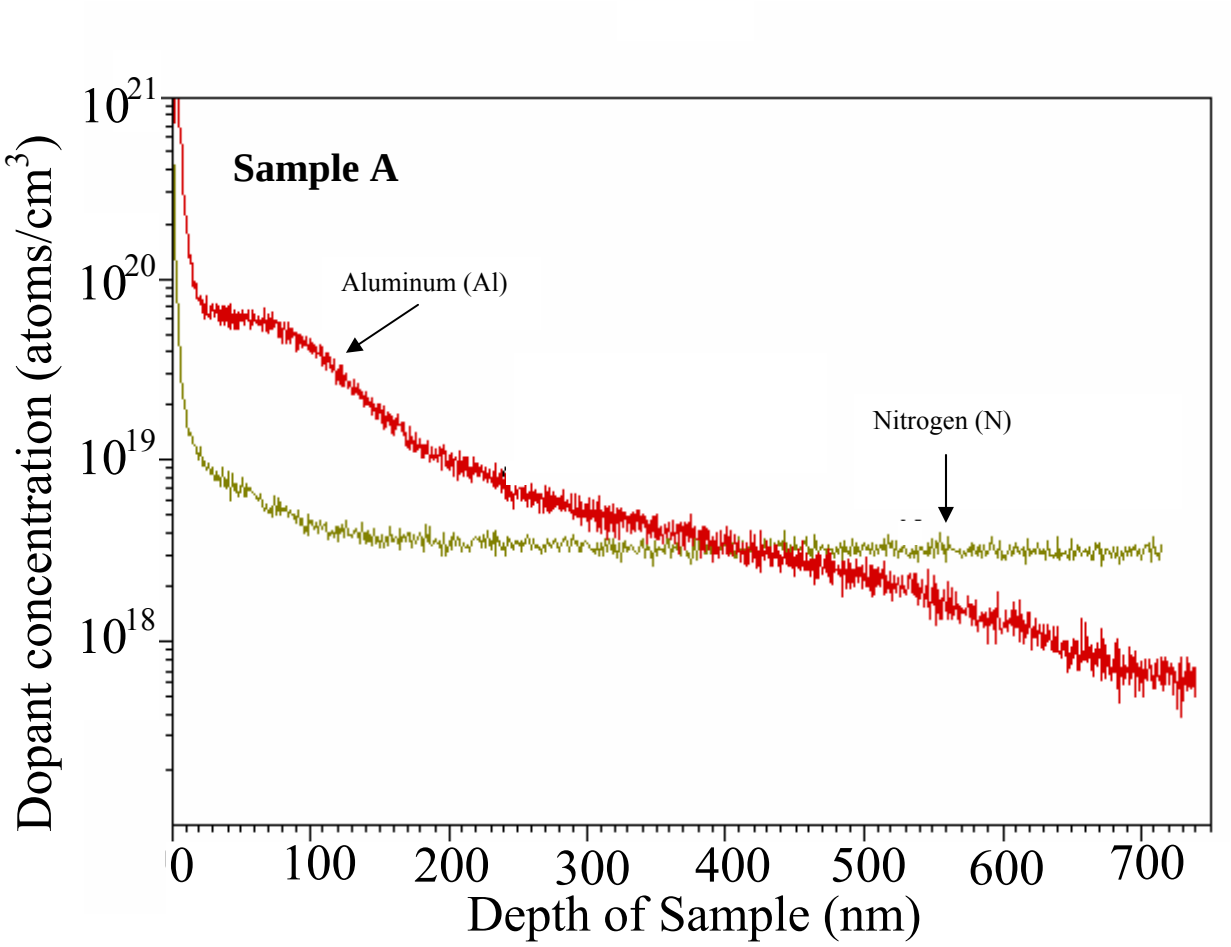

Figure 3. Concentration depth profiles of Aluminum and Nitrogen measured with SIMS for sample A.

The results of SIMS studies are presented in Figs. 3 and 4 which show that the nitrogen (n-dopant) concentration for samples A and B are almost the same, however, there is a noticeable difference in the aluminum (p-dopant) concentration. This difference in the p-dopant concentration can affect the refractive index of the samples because the position of the dopant

level with respect to the conduction band minimum determines the resonance frequency of the electrons. Dopant incorporation into the lattice can influence the motion of the electrons bound to the nucleus and therefore affects the relative permittivity (ε_r) of the material. The refractive index is related to the relative permittivity by the expression $n_s = \sqrt{\varepsilon_r}$ for nonmagnetic materials.

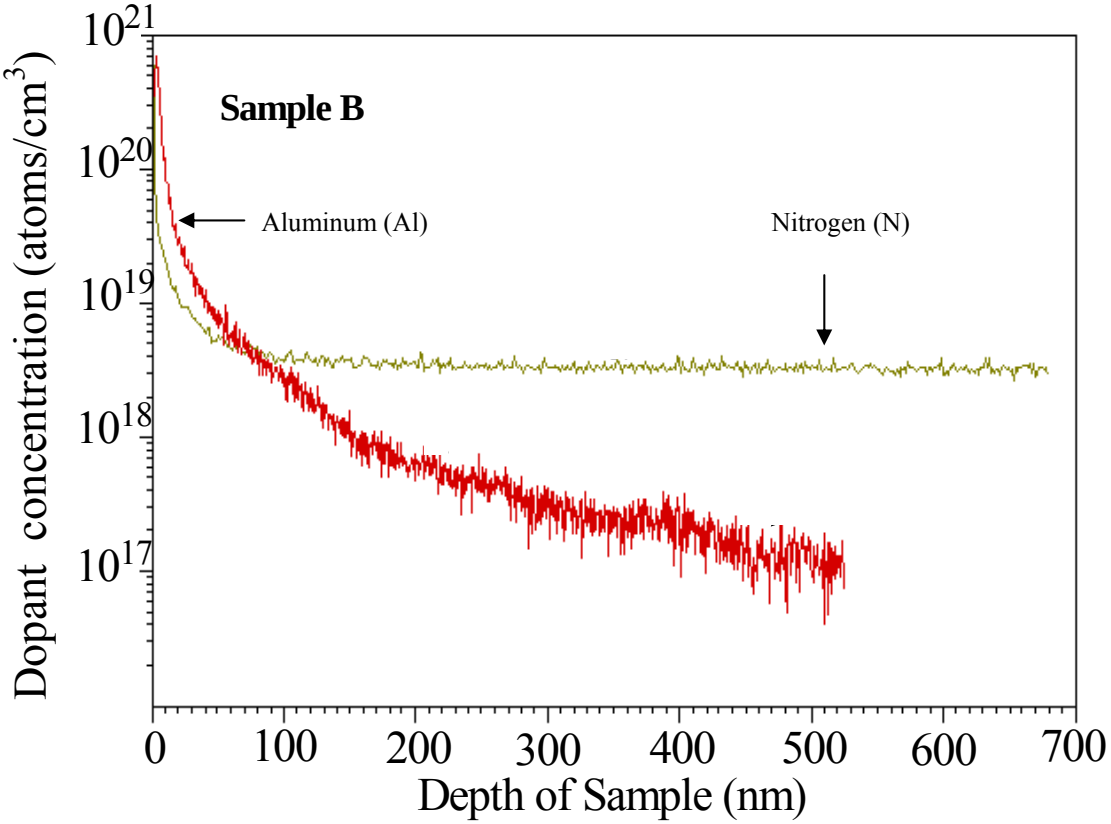

Figure 4. Concentration depth profiles of Aluminum and Nitrogen measured with SIMS for sample B.

Figures 3 and 4 show that the aluminum (p-dopant) concentration profiles differ appreciably along the thickness of the samples. The exact mechanism of how the dopant concentration and temperature affect the optical properties of the SiC chip is not well-understood at this point. But a plausible reason for the effect of temperature on refraction index is that the electrons acquire higher energy at higher temperatures and thus jump from the valance band or

donar level to the conduction band. This increases the electron density in the conduction band, which can affect the optical response of the sensor.

In this section Approach 2 for selective gas sensing is discussed. In Approach 2 selective gas trapping structures including the near surface silicon carbide chip lattice, grain boundaries and vacancies/voids are used for selective gas detection. The species for chemical sensing have been restricted to nitrogen (N_2) and carbon dioxide (CO_2) to demonstrate detection selectivity. An analysis of diffusivity of these species in SiC shows that the diffusion of nitrogen into SiC is over 1000 times faster than the diffusion of oxygen at 1000°C. CO_2 diffusion into SiC is negligible. This differential increases with decreasing temperature. This data suggests that nitrogen selectivity can be controlled by diffusion into the surface layer or a designed epilayer.

G.3 Design and Fabrication of Sensor Optical Interface:

The heart of the gas species sensor measurement system is the non-invasive free-space beam interrogated SiC chip placed as a window in a high temperature high pressure cell exposed to the given gas species. Hence, it is important to understand the mechanical and optical behavior of the SiC chip under high pressures. This study will enable the correct physical design of the chip in terms of its size, thickness, and shape. For symmetry, we assume a circular disk shape.

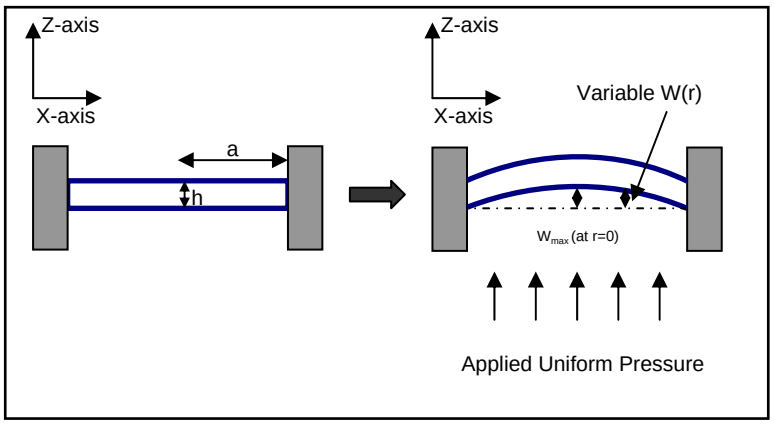

Fig.5 Mechanical Model and Analysis of SiC Chip.

The effect of pressure on the optical chip can be measured by observing spatial two dimensional (2-D) fringes obtained by optical interference of wavefronts reflecting off the front

and back surfaces of the circular optical chip. The circular chip bends under applied pressure (see Figure 5). Since the chip is circular with supported edges, the bending under pressure is symmetrical given by the equation [5]:

$$w(r) = \frac{P(a^2 - r^2)}{64D}\left(\frac{5+\nu}{1+\nu}a^2 - r^2\right) \qquad (1)$$

where w(r) is the bend in chip at a certain radius r, P is applied pressure, 'a' is the radius of the chip, 'υ' is the Poisson's ratio and D is rigidity constant. With 'h' given as the thickness of the chip, E the Young's modulus of the chip, D is in turn defined as [5]:

$$D = \frac{Eh^3}{12(1-\upsilon^2)} \qquad (2)$$

Figure 6 (a), (b), (c) show a series of simulation plots of circular chip under gradually increasing pressure.

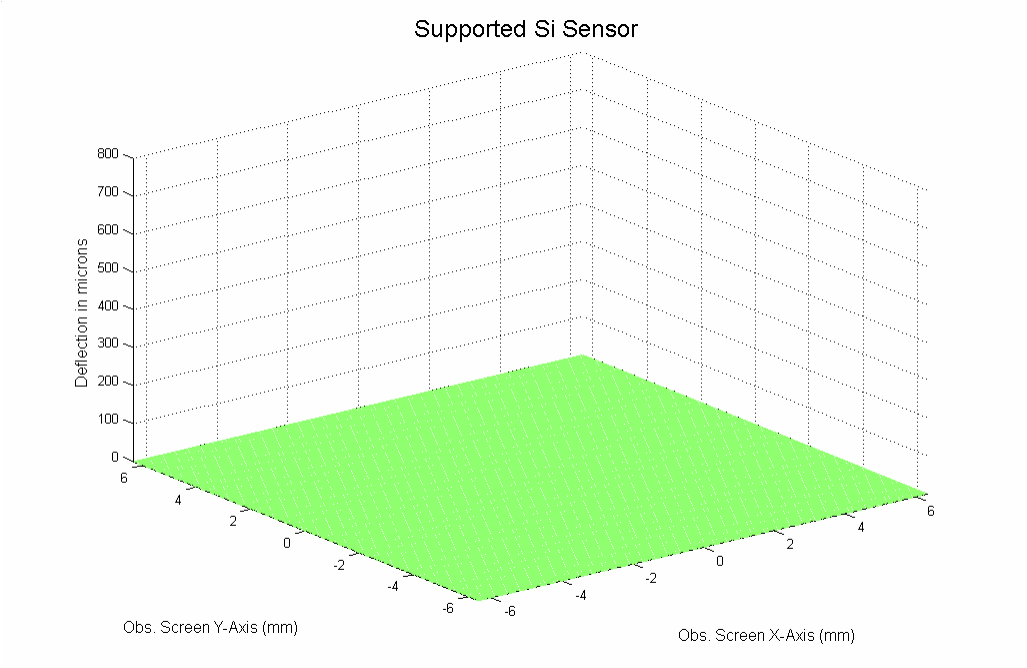

(a)

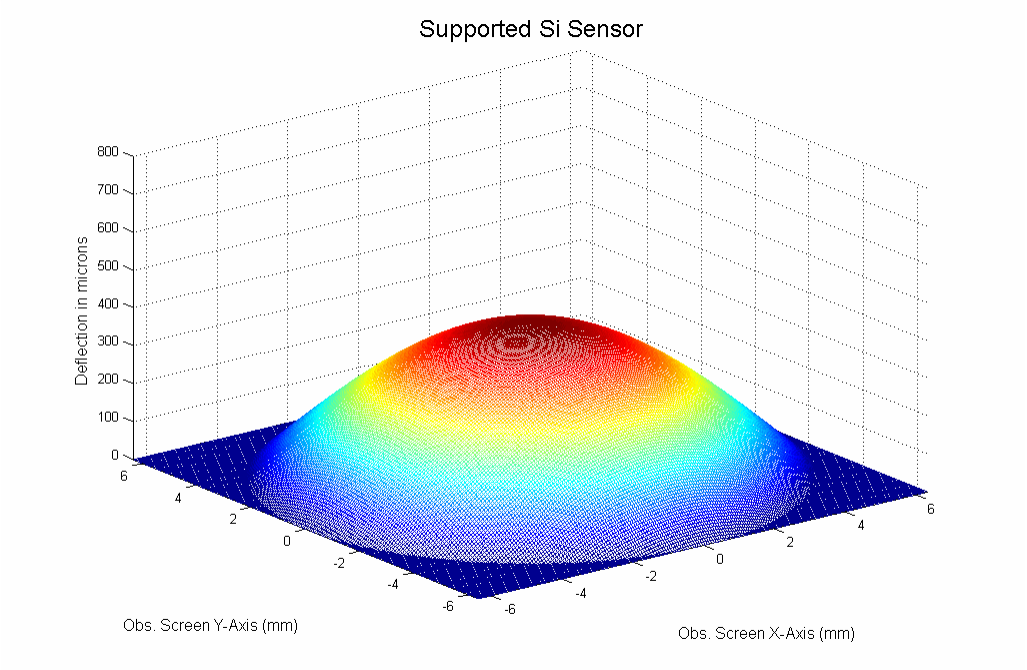

(b)

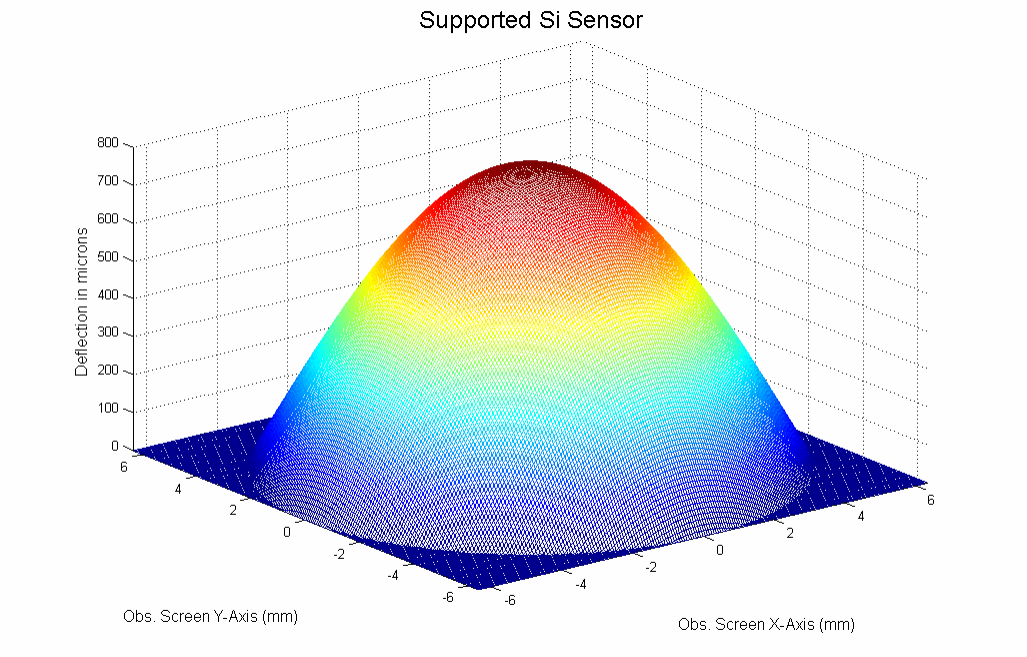

(c)

Fig. 6. Mechanical Deflection of sensor (Si) chip under applied pressure P. (a) P=0; (b) P=10 atm. (c) P=20 atm. Si material mechanical properties listed in references [6,7].

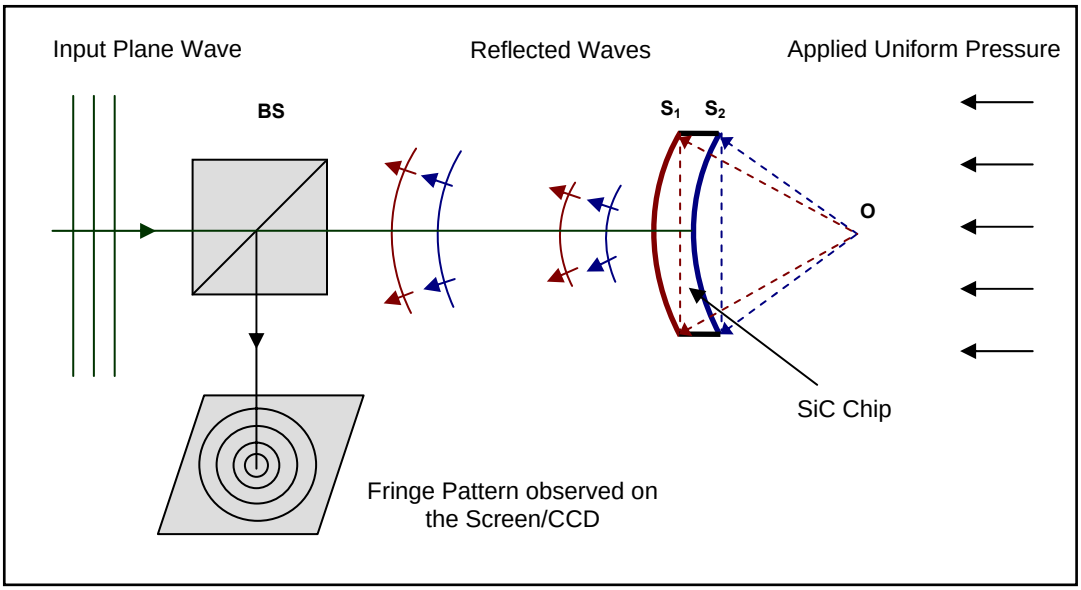

Figure 7. Sensor Chip optical response under applied pressure. S1/S2: Sensor Front/Back Surface; O: Center of Curvature; BS: Beam Splitter.

A plane wavefront falling on the sensor chip gets reflected from the front and back surfaces of the sensor chip and give interference patterns in an observation plane. The nature of fringes depends on the change in curvature of the sensor chip surfaces under applied pressure. When the deflection is small compared to the thickness of the chip, the curvatures of the sensor's surfaces can be approximated as spherical (see Figure 7).

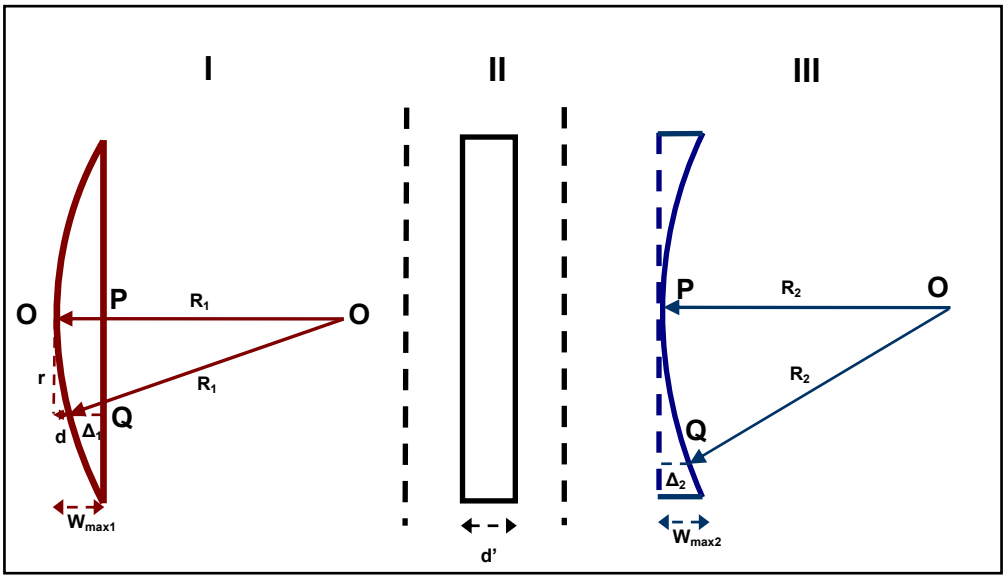

Fig. 8. Phase segments 1,II and III of the optical chip each contributing to the phase difference between the two reflected wavefronts.

Thus, the fringes obtained on the screen are a result of interference between two concentric spherical wavefronts. The two wavefronts travel different distances and as a result gain optical path difference between them. Detailed analysis of phase difference gained over segments of the sensor can be performed by dividing the sensor in three phase segments as shown in Figure 8. The phase gained by rays passing through the optical chip is evaluated in the following segment-by-segment manner.

Segment I Phase: First segment of the sensor acts as a plano-convex lens and the optical path difference gained by rays passing through it is given by δ_1

$$
\begin{aligned}
l_1 &= d - \Delta_1(r) \\
l_1 &= R_1 - \sqrt{R_1^2 - r^2} \\
l_1 &= R_1 - R_1\left(1 - \frac{r^2}{2R_1^2}\right) = \frac{r^2}{2R_1} \qquad (3) \\
\Delta_1(r) &= d - \frac{r^2}{2R_1} \\
\delta_1(r) &= n\Delta_1 = n\left(d - \frac{r^2}{2R_1}\right)
\end{aligned}
$$

where n is the refractive index of the chip and r is the distance from the center of the chip.

Segment II Phase: The second segment 1 of the sensor acts as a mere slab leading to an optical path difference of δ_2.

$$\delta_2 = nd' \qquad (4)$$

Segment III Phase: The third segment of the sensor acts as a concave lens leading to an optical path difference of δ_3.

$$
\begin{aligned}
\Delta_2(r) &= R_2 - R_2\left(1 - \frac{r^2}{2R_2^2}\right) \\
\Delta_2(r) &= \frac{r^2}{2R_2} \qquad (5) \\
\delta_3(r) &= n\Delta_2(r) = n\left(\frac{r^2}{2R_2}\right)
\end{aligned}
$$

Since the wavefront reflecting from the back surface travels through these segments twice the total optical path difference is given as:

$$\delta_t(r) = 2\left[\delta_1(r) + \delta_2 + \delta_3(r)\right]$$
$$\delta_t(r) = 2\left[n\left(d - \frac{r^2}{2R_1} \right) + nd' + n\left(\frac{r^2}{2R_2} \right) \right] \qquad (6)$$
$$\delta_t(r) = 2n\left[\left(d + d'\right) + \left(\frac{r^2}{2R_2} d - \frac{r^2}{2R_1} \right) \right]$$

Since,

$$\left(d + d'\right) = h \qquad (7)$$

where h is the thickness of the optical chip.

$$\delta_t(r) = 2n\left[h + r^2 \left(\frac{1}{2R_2} - \frac{1}{2R_1} \right) \right]$$
$$\delta_t(r) = 2nh + nr^2 \left(\frac{1}{2R_2} - \frac{1}{2R_1} \right) \qquad (8)$$

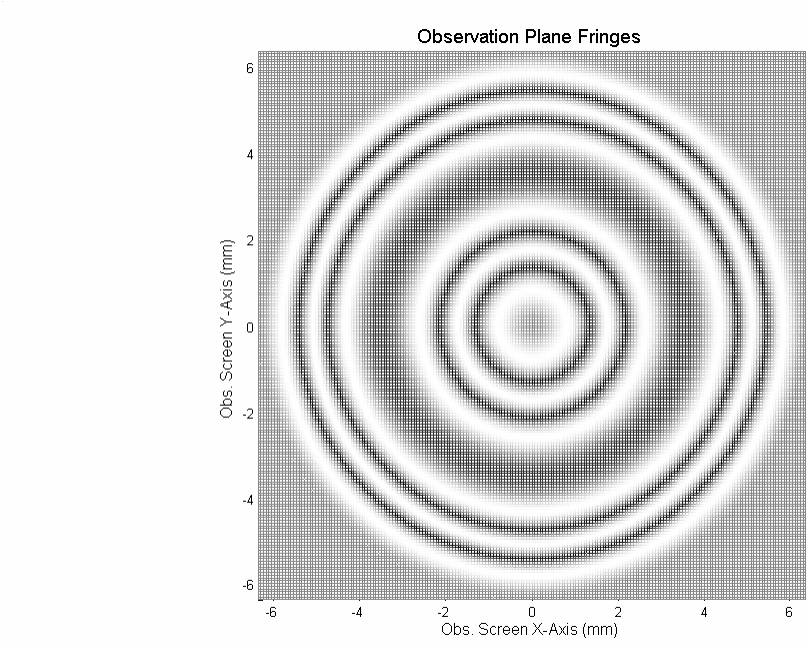

Fig. 9 Theoretical optical Fringes obtained at 20 atm. of pressure with Si optical chip used as the gas cell window.

Figure 9 shows the fringes obtained using the above theoretical expression. Fringe pattern was evaluated at a pressure of 20 atm. for a Silicon optical chip [6-7] with a radius of 6.35 mm (0.5inch diameter) and thickness of 275 μm.

The experimental setup for study for optical fringe variation under pressure is shown in Figure 10(a), (b). The pressure chamber holds the sensor chip at one end with a 0.5 inch diameter orifice where pressure acts on the chip. The rest of the chip is sealed to the supporting plate leading to the mechanical model of deflection of a supported plate under pressure. A C-band tunable IR laser source is used for the setup. The laser beam is expanded by utilizing a pair of spherical lenses of focal length 50 mm and 400mm. The expanded beam passes through a polarization beam splitter. The polarized light gets reflected from the front and back surface of the sensor and the two wavefronts form fringes that are recorded by an IR CCD camera.

In order to study the mechanical performance of the pressure chamber, a copper sheet was used in place of the sensor. The metal sheet being malleable stretched beyond its elastic limits under pressure. The plate stretched out at the desired location indicating the expected behaviour of pressure with radial symmetry. Figure 11 (a), (b) show the copper sheet and the plate that held the copper sheet while it was under pressure.

Initial optical tests were carried out at zero applied pressure. The Silicon chip sensors used showed different results as compared to the expected theoretical results. The theoretical model assumed the two surfaces of the chip to be parallel while there was no pressure applied on the chip. However, the available Si chips had front and back surfaces with thickness as well as tilt variation with respect to each other. This resulted in optical fringes obtained at the observation plane whereas according to theory a fixed irradiance value with zero fringe visibility was expected. (see Figure 12(a)). When pressure is increased to 30psi (about 2 bars), the chip as expected deforms creating another fringe pattern that indicates a specific pressure change. This process enables the chip to provide pressure readings in a non-invasive manner.

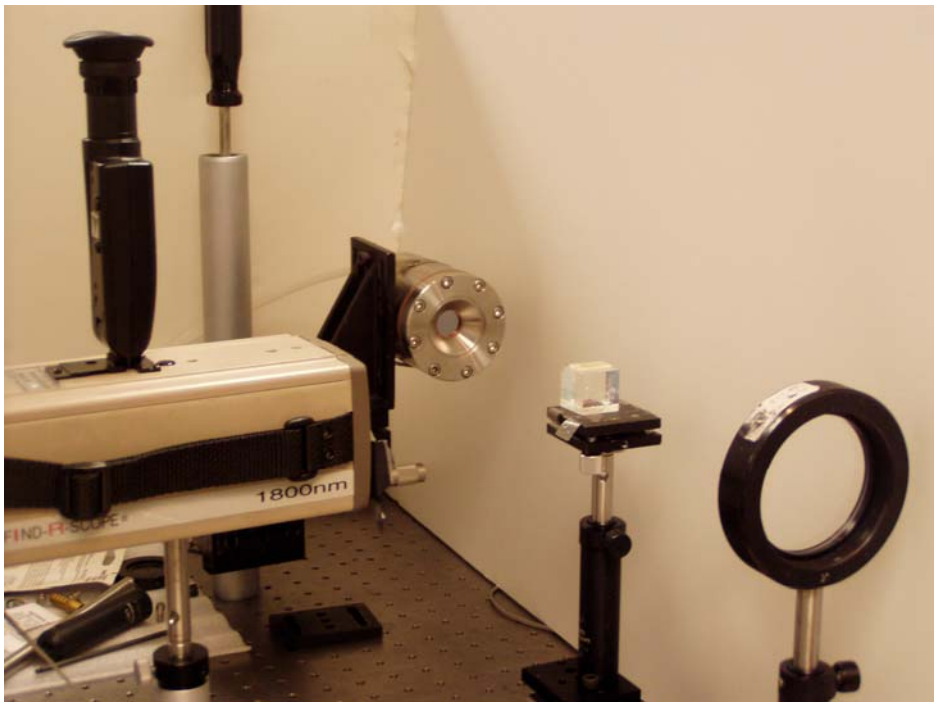

(a)

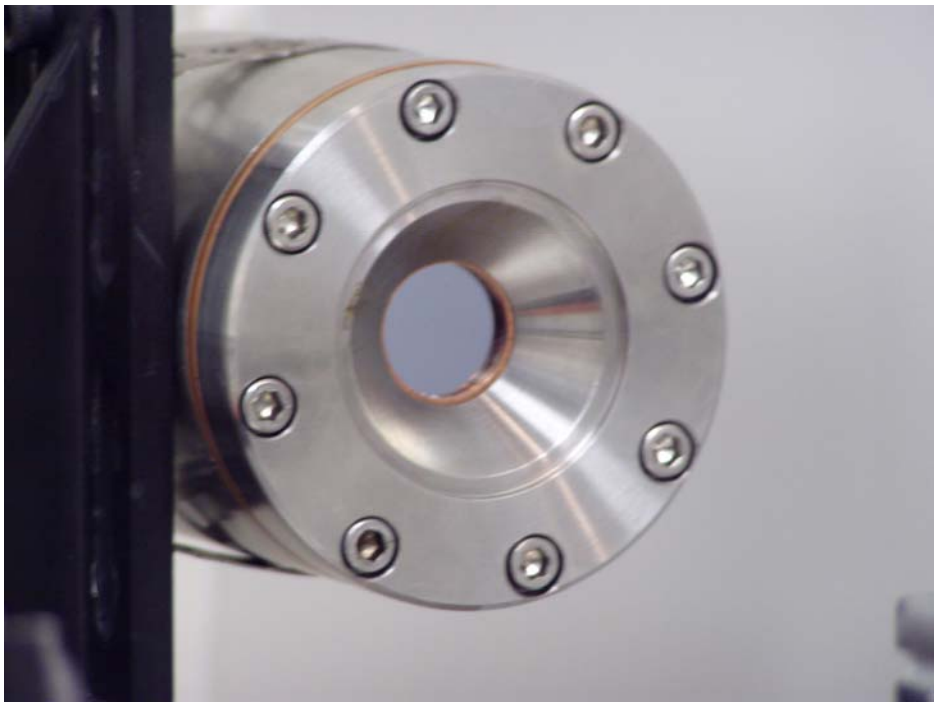

(b)

Figure 10. Front view of the calibration cell with the Si optical chip mounted as the window.

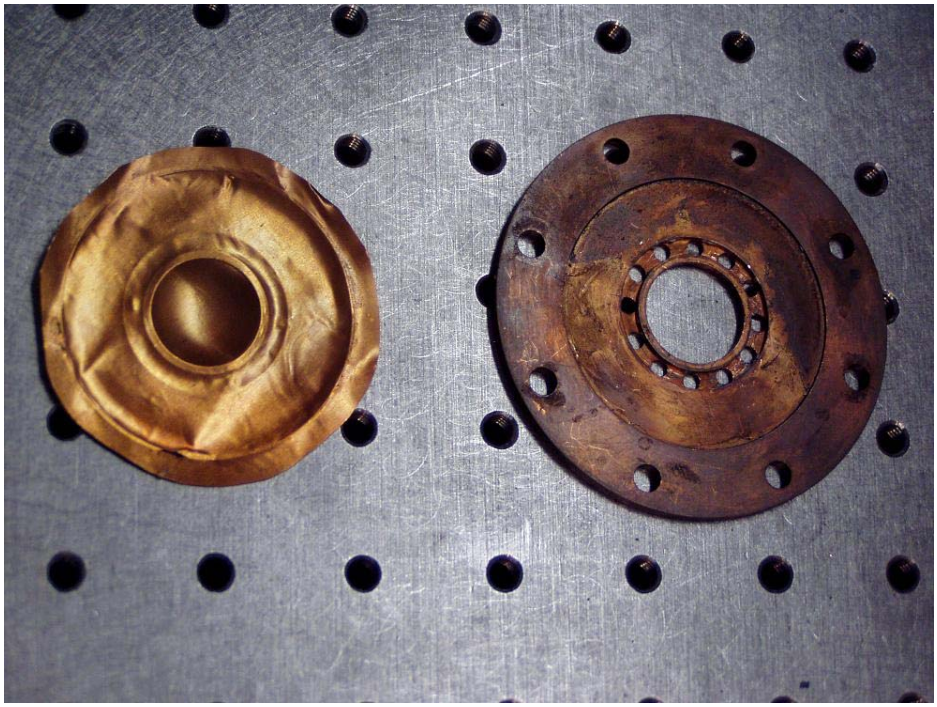

(a)

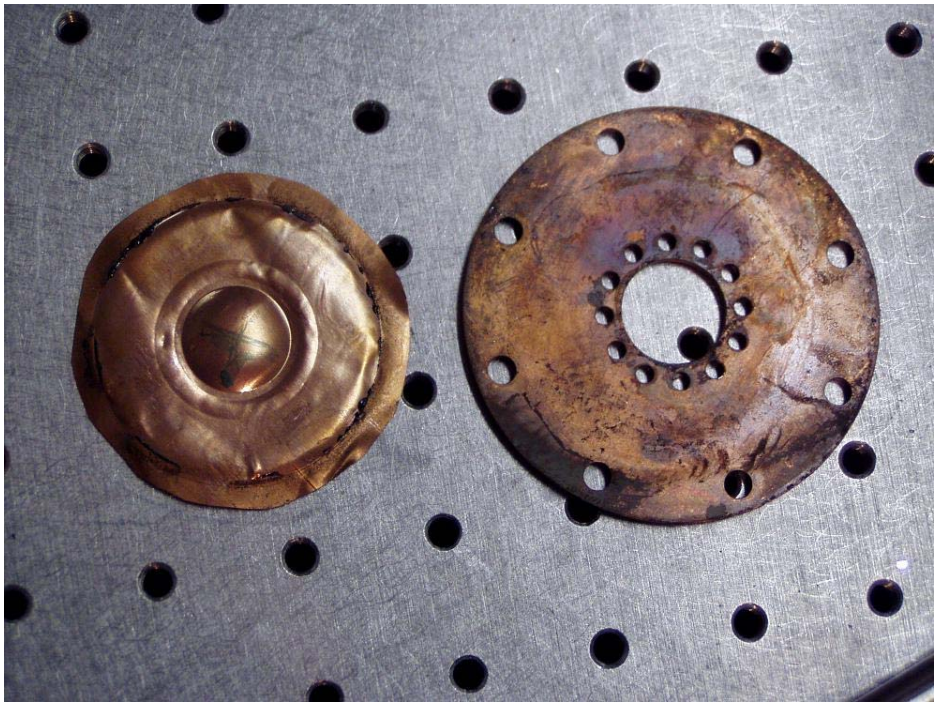

(b)

Figure 11. Thin Copper sheet showing results of pressure test done in the gas calibration cell, along with the supporting/holding plate.

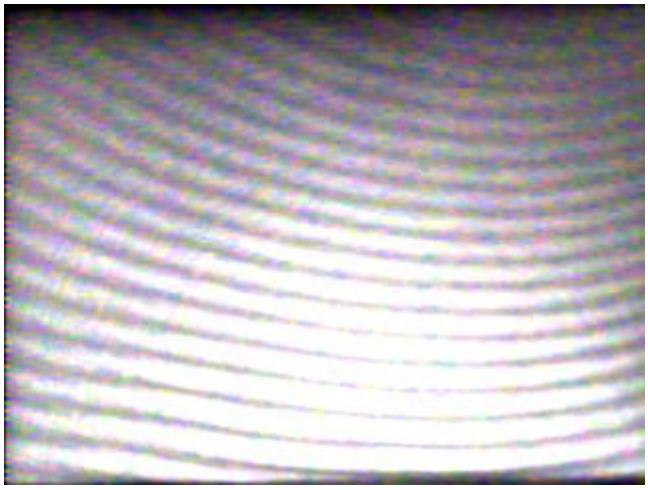

(a)

(b)

Figure12. (a) Due to non-ideal Si chip surface variations, for zero applied pressure fringes were obtained from the optical interface using the Si chip at wavelength of 1550nm. (b) For pressure of 30 psi (about 2 bars), the fringe pattern changes indicating chip deformation.

The deflection equations analysis performed for sensor chip shows the expected deflection behavior under pressure but it does not predict stress failure under high pressure. The sensor chip being brittle breaks when the maximum stress in the chip reaches its failure stress level. For the supported circular plate – type sensor chip the maximum stress in the chip caused by pressure is at the center of the chip given by the equation [5]:

$$(\sigma_r)_{\max} = \frac{3(3+\nu)Pa^2}{8h^2} \qquad (8)$$

where P is the applied pressure, a is the radius of the sensor chip, ν is the Poisson's ratio, and h is the thickness of the sensor chip. The stress failure for Silicon is chosen to be 300 MPa. or equivalently 2961 atm [6-7]. Figure 13 shows how the Silicon sensor chip reaches this stress level with increasing applied pressure for sensor chip radii of 3.175 mm (0.25 inch) and 6.35 mm (0.5 inch). Here chip is 275 micron thick.

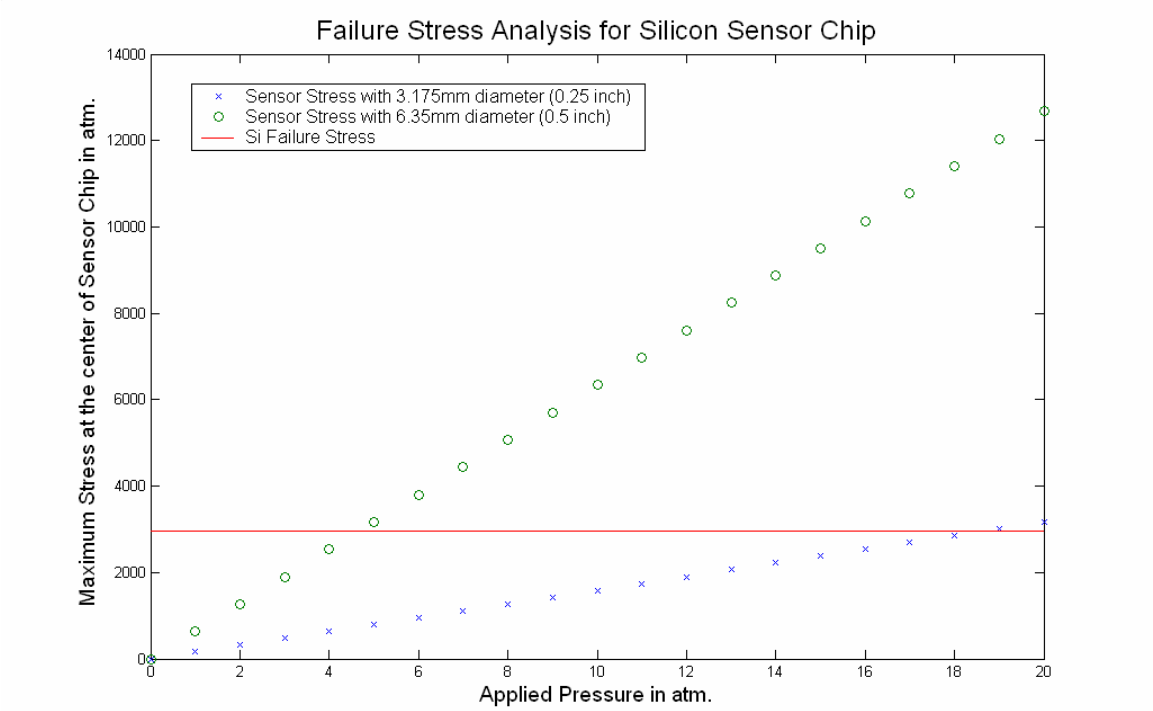

Figure 13. Sensor Chip approaching failure stress level with increasing Pressure

H: RESULTS AND DISCUSSION

The initial results from the built calibration cell indicates that optical chip fixture inserts with smaller apertures and better sealing needs to be designed to avoid substantial deflection of chips (relative to chip thickness) due to pressures reaching 50 bars. In addition, smaller chips sizes can meet the optical flatness tolerances needed for improved resolution fringe analysis using either CCD cameras or point detectors.

Aluminum has been laser doped into 6H-SiC chip to tune the refractive index response to primarily oxygen. Laser doping with nitrogen will be conducted next to simulate refractive index changes for near surface lattice absorption for nitrogen gas sensing.

I: CONCLUSION

In conclusion, this report describes work that have met the two Q1 and Q2 stated objectives of (a) Review Phase I results. Negotiate, award, and initiate Phase II work including delineation of milestones and (b) Complete construction of high temperature high pressure test equipment to permit sensor calibration. Next two quarters will focus on meeting objectives of (c) Complete feasibility assessment of sensor element to detect CH4, CO, and H2 through changes in refractive index and (d) Complete calibration studies for gases to assess sensitivity and detection limits for simple gas mixtures.

J: REFERENCES

[1] R. Duncan, D. Gifford, V. Rajendran, " OFDR tracks temperatures on power generators," Laser Focus World Magazine, p.89, Oct. 2003.

[2] A. D. Kersey, et.al., " Fiber Grating Sensors," IEEE/OSA J. Lightwave Tech., Vol.15, No.8, pp.1442-1463, August 1997.

[3] Brian Culshaw, " Optical Fiber Sensor Technologies: Opportunities and Perhaps Pitfalls," IEEE/OSA Journal of Lightwave Technology, Vol. 22 , No. 1, pp 39 – 50, Jan. 2004.

[4] Michigan State University Project (DE-FG26-01NT41358) (Ref. P. Tobias, B. Golding, R. Ghosh, IEEE Sensors Journal, Vol. 2, No. 5, October 2003).

[5] S. P. Timoshenko and S. Woinowsky-Krieger, Theory of Plates and Shells, pp. 56-57, (McGraw-Hill Inc., New York, NY 1959).

[6] Properties of Silicon, (http://www.design.caltech.edu/Research/MEMS/siliconprop.html).

[7] Fang Yu, Wenbin Sang, Enwen Pang, Donghua Liu, and Jianyong Teng, "Stress Analysis in Silicon Die under Different Types of Mechanical Loading by Finite Element Method (FEM)," IEEE Transactions on Advanced Packaging, Vol. 25, Issue 4, pp. 522-527, Nov. 2002.